Journal of Alloys and Compounds 499 (2010) 68–74

Contents lists available at ScienceDirect

Journal of Alloys and Compounds

journal homepage: www.elsevier.com/locate/jallcom

Thermodynamic properties of Mg_2Si and Mg_2Ge investigated by first principles method

Hanfu Wang*, Hao Jin, Weiguo Chu*, Yanjun Guo

National Center for Nanoscience and Technology of China, Beijing 100190, China

ARTICLE INFO

Article history:
Received 10 August 2009
Accepted 27 January 2010
Available online 4 February 2010

Keywords:
Mg_2Si
Mg_2Ge
Thermal conductivity
Slack's equation
Acoustic Debye temperature

ABSTRACT

The lattice dynamics and thermodynamic properties of Mg_2Si and Mg_2Ge are studied based on the first principles calculations. We obtain the phonon dispersion curves and phonon density of states spectra using the density functional perturbation theory with local density approximations. By employing the quasi-harmonic approximation, we calculate the temperature dependent Helmholtz free energy, bulk modulus, thermal expansion coefficient, specific heat, Debye temperature and overall Grüneisen coefficient. The results are in good agreement with available experimental data and previous theoretical studies. The thermal conductivities of both compounds are then estimated with the Slack's equation. By carefully choosing input parameters, especially the acoustic Debye temperature, we find that the calculated thermal conductivities agree fairly well with the experimental values above 80 K for both compounds. This demonstrates that the lattice thermal conductivity of simple cubic semiconductors may be estimated with satisfactory accuracy by combining the Slack's equation with the necessary thermodynamics parameters derived completely from the first principles calculations.

© 2010 Elsevier B.V. All rights reserved.

1. Introduction

The renaissance of thermoelectric materials since 1990s has motivated extensive studies on low thermal conductivity semiconductors. The thermoelectric efficiency is characterized by figure of merit $ZT = S^2\sigma T/\kappa$, where S, σ, κ and T are Seebeck coefficient, electrical conductivity, thermal conductivity and absolute temperature, respectively. Good thermoelectric materials should have large Seebeck coefficient, high electrical conductivity, and low thermal conductivity. For lightly to moderately doped semiconductors, thermal conductivity is dominated by phonon transport. Numerous theoretical and experimental studies have shown that nanostructures could significantly reduce the lattice thermal conductivity κ_L by increasing phonon scatterings and phonon confinements [1–5]. On the other hand, Morelli et al. recently pointed out that the intrinsically low thermal conductivity can be found in certain semiconductors such as $AgSbTe_2$ and $AgBiSe_2$ [6], which is attributed to the strong anharmonicity of the phonon vibrations in these I–V–VI_2 compounds. This provides an alternative route of developing potential thermoelectrics by intentionally searching for the crystal structures with low thermal conductivity. The thermal conductivity of a semiconductor with a known crystal structure, in principle, can be estimated with the help of theoretical approaches such as molecular dynamics (MD) method. The MD method has been proved to be a powerful tool to determine κ_L of a wide range of solids [7–12]. However, it requires a reliable empirical potential field which is not readily available in most cases. Fortunately, simple empirical models like Slack's equation offer a simple and rapid approach to assess the heat transfer ability of the solids above their Debye temperature [13].

The Slack's equation is given as:

$$\kappa_L = A\frac{\bar{M}\theta_a^3\delta n^{1/3}}{\gamma^2 T} \quad T > \theta_a \tag{1}$$

where $\bar{M}$ (amu) is the average atomic mass, θ_a (K) the acoustic Debye temperature, δ^3 (Å^3) the average volume per atom, n the number of atoms in each primitive cell, γ the high temperature Grüneisen coefficient, $A = 2.43 \times 10^{-6}/(1 - 0.514/\gamma + 0.228/\gamma^2)$ for thermal conductivity in W/m/K.

θ_a and γ in Eq. (1) are two critical thermodynamics parameters that affect the calculated thermal conductivity. In practice, they were often derived from the experimental heat capacity and thermal expansion coefficient, respectively. Since the experimental data are not always available, it is desirable to predict the parameters systematically from some sort of theoretical calculations [13,14].

In this paper, we use magnesium silicide (Mg_2Si) and magnesium germanide (Mg_2Ge) as model systems and estimate their temperature dependent thermal conductivities from the Slack's

* Corresponding authors. Fax: +86 10 62656765.
E-mail addresses: wanghf@nanoctr.cn (H. Wang), hjin@nanoctr.cn (H. Jin), wgchu@nanoctr.cn (W. Chu).

0925-8388/$ – see front matter © 2010 Elsevier B.V. All rights reserved.
doi:10.1016/j.jallcom.2010.01.134

equation based on the thermodynamics parameters derived fully from the first principles calculations.

Mg_2Si and Mg_2Ge are II–IV group semiconductors with an anti-fluorite structure ($FM\bar{3}m$ symmetry). In each of their primitive cell, there are two Mg atoms which are located at $\pm\mu$ ($\mu = \left(\frac{1}{4}, \frac{1}{4}, \frac{1}{4}\right) a$, where a is the lattice constant), and one Si (Ge) atom which occupies the *fcc* (face-centered cubic) site. Mg_2Si and Mg_2Ge are regarded as competitive candidates for thermoelectric applications and have attracted much attention recently [15–18].

Obtaining phonon properties is a key step to calculate the vibrational thermodynamics of the semiconductors. To date there are only a few *ab initio* studies on phonon properties of Mg_2Si and Mg_2Ge. Among them, Baranek et al. calculated the phonon frequencies of Mg_2Si at the Gamma point of the Brillouin zone [19]. Very recently, Tani and Kido performed lattice dynamics calculations on Mg_2Si and Mg_2Ge with the first principles calculations in the framework of density functional theory (DFT) within General Gradient Approximations (GGA) [20]. The calculated heat capacity, Debye temperature, and entropy of the two compounds were found to be in good agreement with the experimental results.

In this work, we further compute the temperature dependent Helmholtz free energy, bulk modulus, thermal expansion coefficient and overall Grüneissen coefficient for Mg_2Si and Mg_2Ge. Based on these calculations, we determine the two important parameters of the Slack's equation, namely, θ_a and γ. By carefully choosing θ_a, we find that the calculated thermal conductivities agree fairly well with the experimental values in a temperature range above 80 K for both Mg_2Si and Mg_2Ge.

2. Computational methods

The structural and phonon properties are calculated based on the DFT method in the framework of local density approximation (LDA) which is implanted in a plane-wave pseudopotential code, ABINIT [21,22]. The LDA pseudopotentials of Mg, Si and Ge in the scheme of Troullier–Martins [22,23] are used in all DFT calculations.

All first principles calculations are performed in the primitive cell containing three atoms. The structures of Mg_2Si and Mg_2Ge are first optimized using a Broyden-Fletcher-Goldfarb-Shanno (BFGS) minimization procedure [24] to obtain the equilibrium lattice constant a_0. An $8 \times 8 \times 8$ Monkhorst–Pack [25] grid is used for Brillouin zone sampling and the plane-wave energy cutoff is set to 50 Hartree.

We then vary the lattice constant of the simulation cell to perform the phonon property calculations using a density functional perturbation theory (DFPT) incorporated in the ABINIT code [26,27]. To perform such calculations, we choose a $6 \times 6 \times 6$ Monkhorst–Pack mesh and a plane-wave energy cutoff of 35 Hartree.

In the quasi-harmonic approximation, the temperature dependent Helmholtz free energy $F(V,T)$ can be written as [14]:

$$F(V,T) = E_s(V) + \int_0^{\omega_{MAX}} \left(\frac{1}{2}\hbar\omega + k_B T \ln[1 - e^{-\hbar\omega/k_B T}]\right) D(\omega, V) d\omega \quad (2)$$

where E_s is the static energy at 0 K, $D(\omega, V)$ is the phonon density of states (PDOS) obtained from the lattice dynamics calculations, V denotes the volume of the simulation cell, ω is the frequency, $\hbar$ is the Planck's constant, k_B represents the Boltzmann's constant. The second term in Eq. (2) reflects the contributions to the Helmholtz free energy from the zero-point motion and thermal excitation of the phonons.

3. Results and discussion

3.1. Phonon properties

The phonon dispersion curves of the optimized Mg_2Si and Mg_2Ge structures are plotted along two high-symmetry lines in the first Brillouin zone (Fig. 1). The general shapes of the dispersion curves are comparable with the previous theoretical study by Tani and Kido [20]. It should be mentioned that the optical phonon branches of Mg_2Si overlap significantly with the longitudinal acoustic (LA) phonon branch, while such overlap is so weak for Mg_2Ge that it can only be observed near the zone boundary along the Γ–X line. This is due to the fact that the atomic mass difference between Mg and Si is smaller than the difference between Mg and Ge.

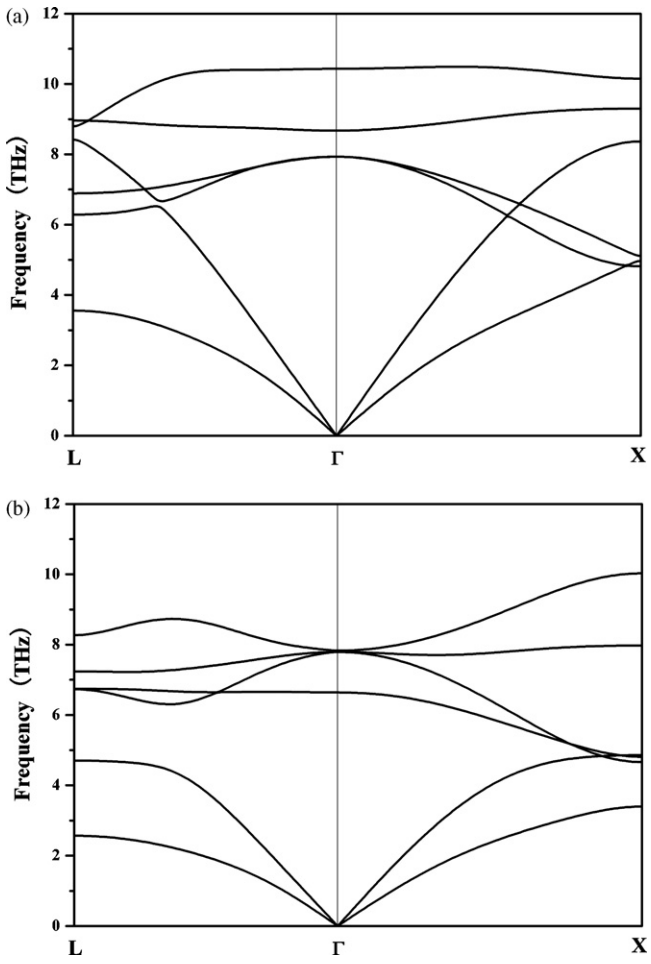

Fig. 1. Calculated phonon dispersion curves of the optimized Mg_2Si (a) and Mg_2Ge (b) structures along two high-symmetry lines in the first Brillouin zone.

In Table 1, the phonon frequencies at several high-symmetry points have been summarized for comparison with the previous theoretical [20] and experimental data [28,29]. Our results which are based on LDA approximation deviate from those obtained from the GGA approximations [20] by 1.3–5.7%, and deviate from the experimental values by 1.2–8.4%. Compared with the LDA calculations performed in this work, the GGA calculations on phonon

Table 1
Phonon frequencies and Debye temperature at high-symmetry points in the first Brillouin Zone for Mg_2Si and Mg_2Ge.

	This work		Literature[c]		Experimental data	
	Mg_2Si	Mg_2Ge	Mg_2Si	Mg_2Ge	Mg_2Si	Mg_2Ge
ω_{TO} (Γ) [THz]	8.67	6.64	8.2	6.4	8.0[d]	6.2[d]
ω_{LO} (Γ) [THz]	10.43	7.83	10.1	7.7	10.56[e] 9.8[d]	8.16[e]
ω_{LA} (X) [THz]	8.37	4.86	8.2	4.8		
$\theta_{a,LA}$ (X)[a] [K]	401.6	233.2				
ω_{TA} (X) [THz]	4.97	3.40	4.7	3.3		
$\theta_{a,TA}$ (X)[a] [K]	238.5	163.1				
$\bar{\theta}_a$(X)[b] [K]	264.1	177.1				
ω_{LA} (L) [THz]	8.42	4.71	8.5	4.8		
ω_{TA} (L) [THz]	3.56	2.57	3.4	2.5		

[a] Obtained using Eq. (9).
[b] Obtained using Eq. (10).
[c] Ref [20].
[d] Ref [28].
[e] Ref [29].

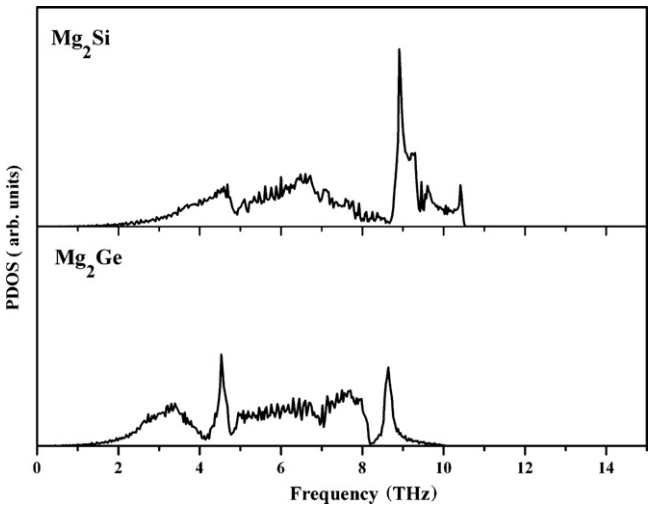

Fig. 2. Phonon density of states spectra of the optimized Mg_2Si (a) and Mg_2Ge (b) structures.

properties show a relatively better agreement with the experimental values. Though the discrepancy between the LDA and GGA calculations on phonon properties has been observed in previous studies [30], we find it has almost no impact on the results of the thermodynamics properties calculations (such as heat capacity, Debye temperature and bulk modulus) in the current work, as we will show in the following sections.

In Fig. 2, the equilibrium phonon density of states $D(\omega, V_0)$ of Mg_2Si and Mg_2Ge are displayed which will be used to compute the heat capacity and Debye temperature curve in section 3.3.

3.2. Equation of state

Fig. 3 displays the Helmholtz free energy of Mg_2Si and Mg_2Ge as a function of average atomic volume at five different temperatures. At a given temperature T, we fit the $F(V,T)$ values obtained at different volumes to a third-order Birch–Murnaghan equation of state (EOS) [31]:

$$F(V(T),T) = F_0(T) + \frac{9}{8}K(T)V_0(T)\left[\left(\frac{V_0(T)}{V(T)}\right)^{2/3} - 1\right]^2 \left\{1 + \left(\frac{4 - K'(T)}{2}\right)\left[1 - \left(\frac{V_0(T)}{V(T)}\right)^{2/3}\right]\right\} \quad (3)$$

where $K(T)$ represents the bulk modulus, $K'(T)$ is the pressure derivative of the bulk modulus. The fitting results are plotted in Fig. 3 as dashed lines. The minimum value of each curve is corresponding to $F_0(T)$ which is denoted as equilibrium Helmholtz free energy at a given temperature T. All data in Fig. 3a and b are referred to the equilibrium Helmholtz free energy of Mg_2Si and Mg_2Ge at 0 K, respectively. From the fitting procedure, one can get several equilibrium properties of the compounds such as $F_0(T)$, lattice constant $a(T)$, $K(T)$ and $K'(T)$.

Fig. 4 displays the equilibrium Helmholtz free energy of Mg_2Si and Mg_2Ge versus temperature. It can be seen clearly that the equilibrium Helmholtz free energy of Mg_2Ge decays faster than that of Mg_2Si as the temperature increases.

The equilibrium lattice constants $a_0(T)$ of Mg_2Si and Mg_2Ge are plotted in Fig. 5a. At 0 K, the lattice constants are 6.29 Å and 6.32 Å for Mg_2Si and Mg_2Ge, respectively. The values are very close to those obtained from the BFGS optimization procedure in this work. They are also comparable with the GGA results and experimental values as shown in Table 2.

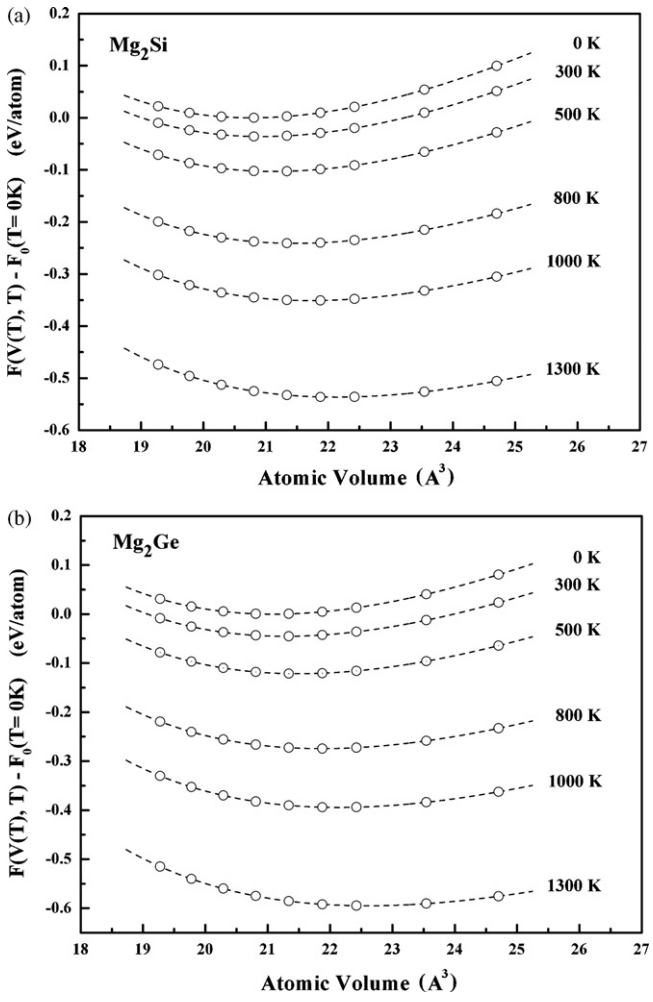

Fig. 3. Helmholtz free energy of Mg_2Si (a) and Mg_2Ge (b) as a function of average atomic volume at several temperatures. The empty circles denote the data evaluated from Eq. (2); The dashed lines represent the fits to the third-order Birch–Murnaghan equation of state. The data in (a) and (b) are referred to the equilibrium Helmholtz free energy at 0 K of Mg_2Si and Mg_2Ge, respectively.

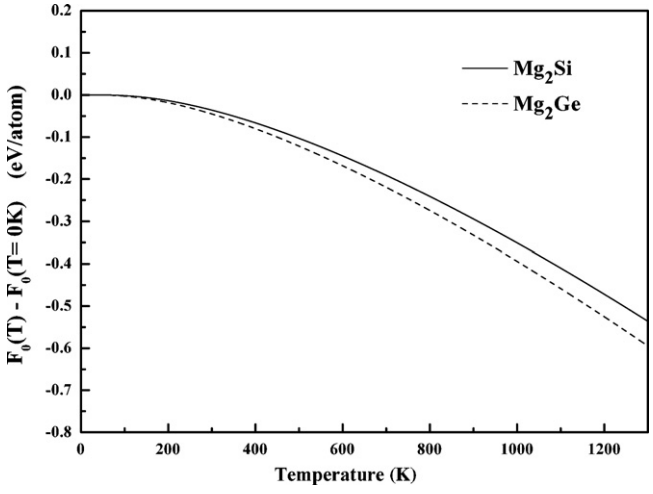

Fig. 4. Equilibrium Helmholtz free energy of Mg_2Si (solid line) and Mg_2Ge (dashed line) as a function of temperature. The data are referred to the equilibrium Helmholtz free energy at 0 K of Mg_2Si and Mg_2Ge, respectively.

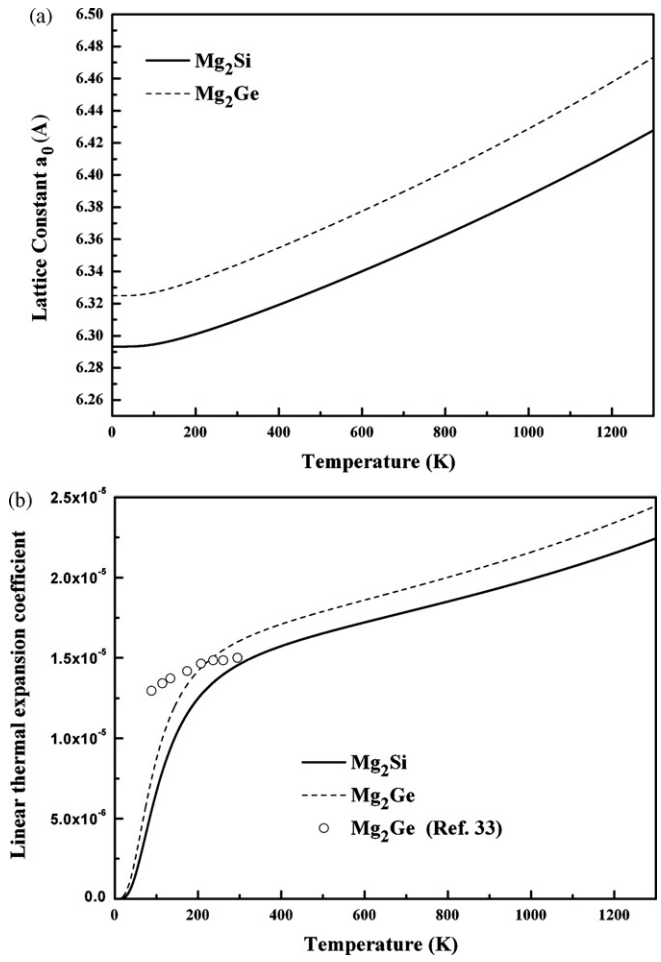

Fig. 5. Lattice constant (a) and linear thermal expansion coefficient (b) of Mg_2Si (solid line) and Mg_2Ge (dashed line) as a function of temperature. The empty circles represent the experimental values of Mg_2Ge.

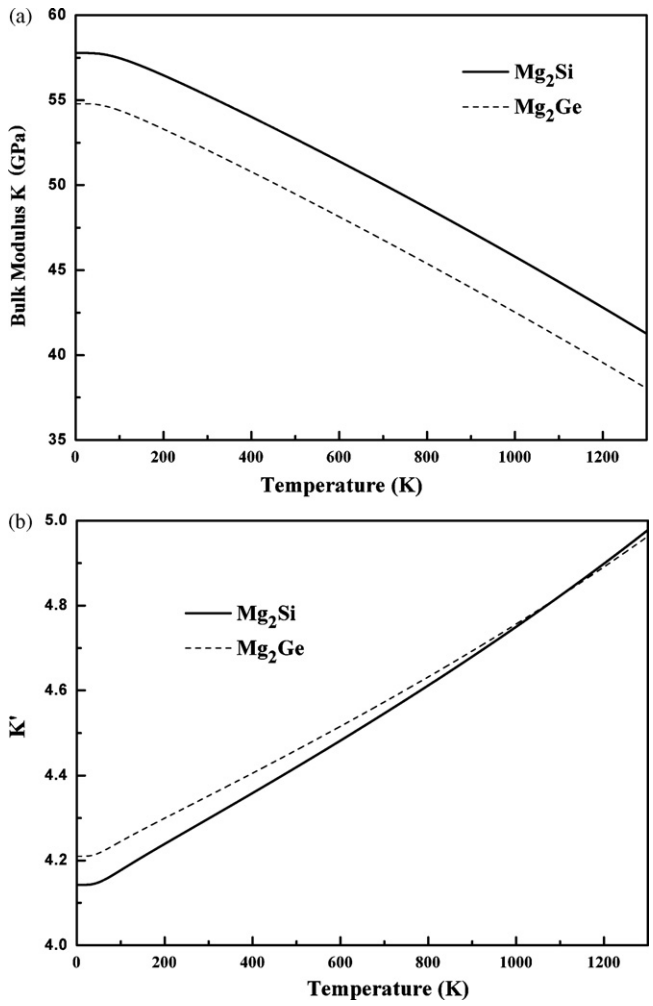

Fig. 6. Bulk modulus $K(T)$ (a) and pressure derivative of the bulk modulus $K'(T)$ of Mg_2Si (solid line) and Mg_2Ge (dashed line) as a function temperature.

The linear thermal expansion coefficients is given as:

$$\alpha_l(T) = \frac{1}{a(T)}\frac{da(T)}{dT} \quad (4)$$

Fig. 5b illustrates the variation of the thermal expansion coefficients of Mg_2Si and Mg_2Ge with the temperature. In the whole temperature range (0–1300 K), the thermal expansion coefficient of Mg_2Si is smaller than that of Mg_2Ge. To our knowledge, no experimental measurement on thermal expansion coefficient of Mg_2Si is available hitherto. The volume thermal expansion coefficient α_V of Mg_2Si was estimated to be 3.27×10^{-5}/K at 300 K [32] which is equivalent to a linear thermal expansion coefficient of $\alpha_l = 1.1 \times 10^{-5}$/K. The result is comparable with the value of 1.4×10^{-5}/K which is obtained in the present work. The linear thermal expansion coefficient Mg_2Ge has been measured from 80–300 K by Chung et al. using a resistance strain-gauge method [33] as illustrated in Fig. 5b. The experimental linear thermal expansion coefficient of Mg_2Ge at 300 K is about 1.5×10^{-5}/K which is comparable with our calculated value of 1.6×10^{-5}/K. However, the agreement between the experimental and theoretical data is quite poor below 150 K. The disparity may need further experimental clarifications by using more accurate measurement techniques, such as variable temperature X-ray diffraction method.

Table 2
Structural and elastic properties of Mg_2Si and Mg_2Ge.

	This work (0 K)		Literature[c] (0 K)		Experimental data[d]	
	Mg_2Si	Mg_2Ge	Mg_2Si	Mg_2Ge	Mg_2Si	Mg_2Ge
a_0 (Å)	6.28[a] 6.29[b]	6.31[a] 6.32[b]	6.295	6.318	6.338	6.393
K (GPa)	57.8	54.8	56.2	55.1	59	54.6

[a] Obtained from the BFGS procedure.
[b] Obtained from the fitting procedure using the Birch–Murnaghan equation of state.
[c] Ref. [20].
[d] Ref. [34].

The bulk moduli of Mg_2Si and Mg_2Ge are plotted in Fig. 6a versus the temperature. The calculated bulk moduli of both compounds at 0 K are in good agreement with the previous theoretical [20] and experimental values [34] (Table 2). In a temperature range of 0–1300 K, the bulk moduli of the compounds decrease with temperature and the bulk moduli of Mg_2Ge are always smaller than that of Mg_2Si. On the other hand, the pressure derivative of the bulk modulus $K'(T)$ is found to increase with temperature for both compounds (Fig. 6b). At 0 K, $K'(T)$ of Mg_2Si is smaller than that of Mg_2Ge. As the temperature increases, $K'(T)$ of Mg_2Si grows more rapidly and exceeds that of Mg_2Ge around 1093 K.

3.3. Specific heat and Debye temperature

The specific heat at constant volume C_v can be computed from the equilibrium PDOS $D(\omega,V_0)$ in the quasi-harmonic approxi-

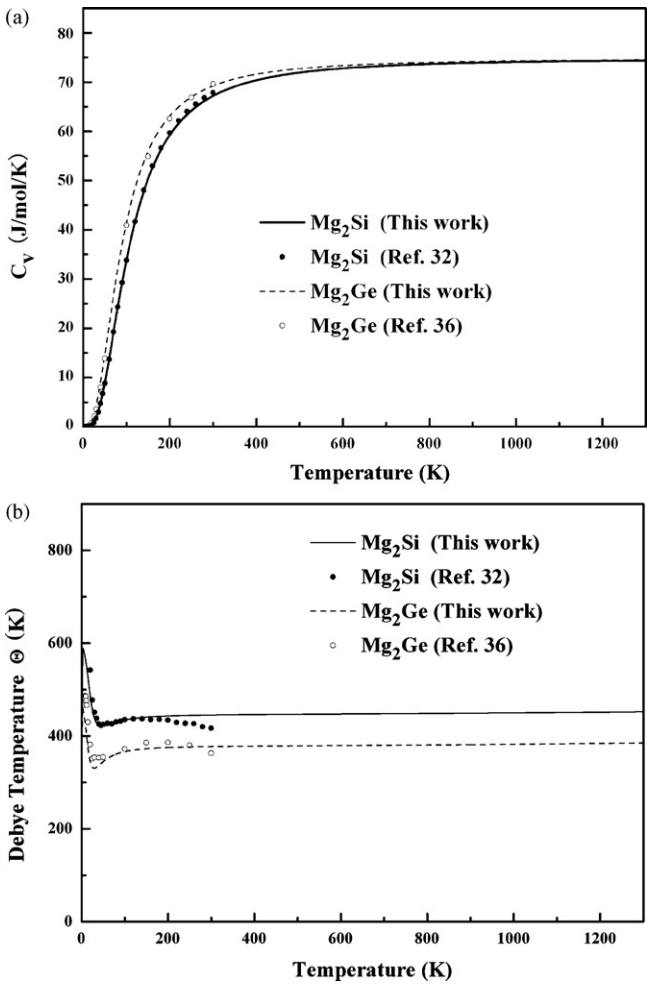

Fig. 7. Constant volume specific heat (a) and Debye temperature (b) of Mg_2Si (solid line) and Mg_2Ge (dashed lines) as a function of temperature. Experimental data (solid circles for Mg_2Si, empty circles for Mg_2Ge) are also displayed for comparison.

mation:

$$C_V = 9R\int_0^{\omega_{MAX}} \left(\frac{\hbar\omega}{k_B T}\right)^2 \frac{e^{\hbar\omega/k_B T}}{(e^{\hbar\omega/k_B T}-1)^2} D(\omega, V_0)d\omega \quad (5)$$

where R is the real gas constant.

We compare the calculated specific heat with the experimental values [32,36] in Fig. 7a in which fairly good agreement can be observed. Our results based on the LDA calculations are also consistent with the previous GGA calculations by Tani and Kido [20]. For example, the specific heats at 300 K are calculated to be 67.2 J/mol/K and 69.2 J/mol/K for Mg_2Si and Mg_2Ge, respectively in the present work, and 67.6 J/mol/K and 69.8 J/mol/K, respectively in Ref. [20].

The Debye temperature can be deduced from the known specific heat data. In the classical Debye model, the specific heat of the bulk is given as [35]:

$$C_V^D(T) = 9R\left(\frac{T}{\Theta_D(T)}\right)^3 \int_0^{\Theta_D(T)/T} \frac{x^4 e^x}{(e^x-1)^2}dx \quad (6)$$

where $\Theta_D(T)$ is the Debye temperature.

$\Theta_D(T)$ can be solved numerically by equating $C_V(T)$ of Eq. (1) with $C_V^D(T)$ of Eq. (6). At a given temperature T, $\Theta_D(T)$ in Eq. (6) is continuously varied as a parameter to calculate $C_V^D(T)$ until $C_V^D(T)$ equals to $C_V(T)$. The final value of $\Theta_D(T)$ is the Debye temperature at the temperature T. The calculated Debye temperatures agree well with the experimental data (Fig. 7b) for both compounds. Note that $\Theta_D(T)$ decreases with the temperature in the very low temperature region. As the temperature increases, $\Theta_D(T)$ increases again and therefore produces a curve minimum. The minimum is crucial for determining the acoustic Debye temperature of the Slack's equation in this study, which will be discussed later in Section 3.5. The experimental Debye temperature curve around the minimum point is reproduced well by the calculated curve, especially for Mg_2Si, which reflects the accuracy of the calculated PDOS.

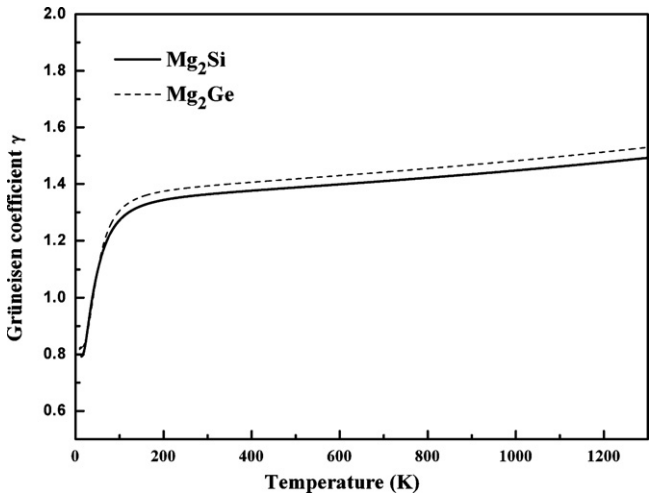

Fig. 8. Overall Grüneisen coefficient of Mg_2Si (solid line) and Mg_2Ge (dashed line) as a function of temperature.

3.4. Overall Grüneisen coefficient

The Grüneisen coefficient is an important parameter to characterize the anharmonicity of the lattice vibrations. The overall Grüneisen coefficient is determined from the linear thermal expansion coefficient, bulk modulus and specific heat and molar volume $V_m(T)$:

$$\gamma(T) = \frac{3\alpha_l(T)K(T)V_m(T)}{C_v(T)} \quad (7)$$

The values of γ of Mg_2Si and Mg_2Ge are compared with each other in Fig. 8. Below 100 K, γ of both compounds increases quickly with the temperature. As the temperature increases further, γ stays almost constant and the value of Mg_2Si is about 2% larger than that of Mg_2Ge in the plateau region.

3.5. Thermal conductivity

For the lightly to moderately doped semiconductors in which defects scattering and boundary scattering do not exist, the Umklapp mechanism is the most important factor to determine the thermal conductivity above the Debye temperature. The intrinsic thermal conductivity in this case can be well described by the Slack's equation.

To apply the equation, the acoustic Debye temperature and Grüneisen parameter are two important parameters that need to be determined carefully. Among them, θ_a is more critical since the thermal conductivity κ_L in Eq. (1) is proportional to θ_a^3. There have been several approaches proposed for calculating the acoustic Debye temperature θ_a. For example, Domb and Salter suggested the following expression [37]:

$$\theta_a{}^2 = \frac{5\hbar^2}{3k_B^2}\frac{\int_0^\infty \omega^2 D_a(\omega)d\omega}{\int_0^\infty D_a(\omega)d\omega} \quad (8)$$

where $D_a(\omega)$ is the acoustic portion of phonon density of states. Theoretically, the overall phonon density of states can be calculated

Table 3
The values of the Slack's equation parameters for Mg_2Si and Mg_2Ge.

	$\overline{M}$ (amu)	δ (Å)	n	$\bar{\theta}_a$ (K)	$\gamma(\bar{\theta}_a)$	$\theta_{a,min}$ (K)	$\gamma(\theta_{a,min})$
Mg_2Si	25.6	2.74	3	264.1	1.36	292.3	1.36
Mg_2Ge	40.4	2.76	3	177.1	1.37	229.3	1.38

routinely based on the lattice dynamics calculations with the aid of modern *ab initio* computational packages. However, the acoustic bands and optical bands are often overlapped with each other in many materials, extracting the acoustic phonon density of states is not a straightforward procedure from a theoretical point of view.

Another relatively simple way is based on the phonon dispersion curve. One can define Debye temperature for each branch of the acoustic phonon modes, namely one longitudinal mode (L) and two transverse modes (T1 and T2), at the zone boundary [38]:

$$\theta_{a,i} = \frac{\hbar\omega_{a,i}}{k_B} \tag{9}$$

where $\omega_{a,i}$ is the frequency of ith (i = L, T1, T2) acoustic mode at the zone boundary. The average acoustic mode Debye temperature $\bar{\theta}_a$ is then given by [38]:

$$\frac{1}{\bar{\theta}_a^3} = \frac{1}{3}\left[\frac{1}{\theta_{a,L}^3} + \frac{1}{\theta_{a,T1}^3} + \frac{1}{\theta_{a,T2}^3}\right] \tag{10}$$

We have utilized this method (denoted method A hereafter) to calculate the average acoustic Debye temperature at X point of the first Brillouin zone $\bar{\theta}_a$(X) for Mg_2Si and Mg_2Ge which are listed in Table 1.

Recently, Bruls et al. suggested to estimate the acoustic Debye temperature from the value at the minimum of the Debye temperature–temperature curve [39,40]. It was proposed based on the following argument. In the very low temperature, the Debye temperature–temperature curve is dominated by the acoustic phonon modes and the Debye temperature decreases with the temperature at the beginning. As the temperature increases, the decrease of the acoustic phonon contribution and the excitation of the optical phonon modes lead to an increase of the Debye temperature. The minimum value Θ_{min} thus represents a good approximation for the high temperature limit of the Debye temperature associated with the acoustic phonons.

From Fig. 7b, $\Theta_{D,min}$ is found to be 421.5 K and 330.7 K for Mg_2Si and Mg_2Ge, respectively. $\Theta_{D,min}$, which is deduced from specific heat, is related to the acoustic Debye temperature of Eq. (1) by [13]:

$$\theta_{a,min} = \Theta_{D,min} \cdot n^{-1/3} \tag{11}$$

In this following, the above procedure is termed method B.

The Grüneisen coefficient γ is used to account for the deviation of the lattice vibration from the anharmonicity. In principle, γ should be contributed from all the acoustic phonon modes in the first Brillouin zone at a temperature close to Debye temperature [13]. In this study, we use the Grüneisen coefficient at the acoustic Debye temperature as the input parameter of the Slack's equation. As the temperature increases from $\bar{\theta}_a$ or $\theta_{a,min}$ to 1300 K (Note that the melting points of Mg_2Si and Mg_2Ge are 1363 K and 1391 K, respectively.), the variation of the Grüneisen coefficient is less than 12% for both compounds (Fig. 8). The observation implies that the contribution of the optic phonon modes to the overall Grüneisen parameter do not change too much with temperature above $\bar{\theta}_a$ or $\theta_{a,min}$.

Table 3 summarizes all necessary input parameters for calculating the thermal conductivity using the Slack's equation. Two sets of the acoustic Debye temperature and the Grüneisen parameter are listed: $\bar{\theta}_a$ and $\gamma(\bar{\theta}_a)$ are associated with the method A, $\theta_{a,min}$ and $\gamma(\theta_{a,min})$ with the method B. It should be noted that the γ values of Mg_2Si and Mg_2Ge are very close to each other, no matter how γ is obtained.

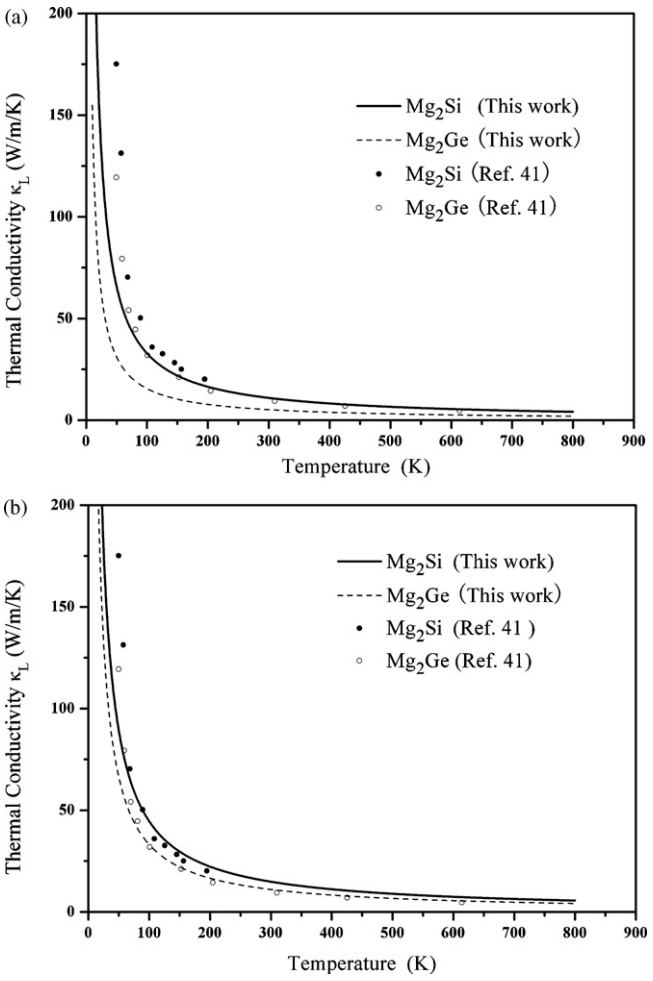

Fig. 9. Thermal conductivity of Mg_2Si (solid line) and Mg_2Ge (dashed lines) which are calculated from the Slack's equation based on the method A (a) and the method B (b). Experimental data (solid circles for Mg_2Si, empty circles for Mg_2Ge) are also displayed for comparison.

We first calculate the thermal conductivity of the two compounds using $\bar{\theta}_a$ and $\gamma(\bar{\theta}_a)$. The results are plotted in Fig. 9a to compare with the experimental data [41]. Though the trend that the thermal conductivity of Mg_2Si is larger than that of Mg_2Ge has been reproduced, the calculation significantly underestimates the thermal conductivity of Mg_2Ge in the low temperature region.

We then employ $\theta_{a,min}$ and $\gamma(\theta_{a,min})$ to perform the same calculation. Fig. 9b shows that the thermal conductivities are in good agreement with the experimental data above 80 K, especially for Mg_2Ge. The major difference between method A and method B comes essentially from the acoustic Debye temperature that is used in the calculation. In the method B, the acoustic Debye temperature is associated with the minimum value in the Debye temperature–temperature curve. This treatment leads to a good agreement between the calculated thermal conductivities and the experimental results above 80 K for Mg_2Ge, but also below $\theta_{a,min}$ for both Mg_2Si and Mg_2Ge. Our study suggests that the lattice thermal conductivity of simple cubic semiconductors may be estimated satisfactorily by using the Slack's equation in conjunction with the necessary thermodynamics parameters derived fully from the first principles calculations.

4. Conclusions

In this work, we calculate the temperature dependent Helmholtz free energy, bulk modulus, thermal expansion coefficient, Debye temperature and overall Grüneisen coefficient of Mg_2Si and Mg_2Ge. By carefully choosing the input parameters of the Slack's equation, especially the acoustic Debye temperature, we find that the estimated thermal conductivities agree fairly well with the experimental results in the temperature range above 80 K. The current study shows that the lattice thermal conductivity of simple cubic semiconductors, like Mg_2Si and Mg_2Ge, may be estimated with satisfactory accuracy by combining the Slack's equation with the necessary thermodynamics parameters derived completely from the first principles calculations.

Acknowledgments

This work is sponsored by the Scientific Research Foundation for the Returned Overseas Chinese Scholars, State Education Ministry of China, and the Knowledge Innovation Program of the Chinese Academy of Sciences (Grant No. KJCX2-YW-H20).

References

[1] A. Balandin, K.L. Wang, Phys. Rev. B 58 (1998) 1544.
[2] R. Venkatasubramanian, Phys. Rev. B 61 (2000) 3091.
[3] J. Zou, A. Balandin, J. Appl. Phys. 89 (2001) 2932.
[4] D. Li, Y. Wu, P. Kim, L. Shi, P. Yang, A. Majumdar, Appl. Phys. Lett. 83 (2003) 2934.
[5] A.I. Hochbaum, R. Chen, R.D. Delgado, W. Liang, E.C. Garnett, M. Najarian, A. Majumdar, P. Yang, Nature 451 (2008) 163.
[6] D.T. Morelli, V. Jovovic, J.P. Heremans, Phys. Rev. Lett. 101 (2008) 035901.
[7] J. Li, L. Porter, S. Yip, J. Nucl. Mater. 255 (1998) 139.
[8] S.G. Volz, G. Chen, Phys. Rev. B 61 (2000) 2651.
[9] P.K. Schelling, S.R. Phillpot, P. Keblinski, Phys. Rev. B 65 (2002) 144306.
[10] F. Müller-Plathe, J. Chem. Phys. 106 (1997) 6082.
[11] P. Jund, R. Jullien, Phys. Rev. B 59 (1999) 13707.
[12] N. Papanikolaou, J. Phys.: Condens. Matter 20 (2008) 135201.
[13] D.T. Morelli, G.A. Slack, in: S. Shinde, J. Goela (Eds.), High Thermal Conductivity Materials, Springer-Verlag, New York, 2005, p. 37.
[14] C.M. Fang, G.A. de Wijs, J. Phys.: Condens. Matter 16 (2004) 3027.
[15] L.M. Zhang, Y.G. Leng, H.Y. Jiang, L.D. Chen, T. Hirai, Mater. Sci. Eng. B 86 (2001) 195.
[16] J.-I. Tani, H. Kido, Physica B 364 (2005) 218.
[17] C.-H. Lee, S.-H. Lee, S.-Y. Chun, S.-J. Lee, J. Nanosci. Nanotechnol. 6 (2006) 3429.
[18] R. Saravanan, M.C. Robert, J. Alloys Compd. 479 (2009) 26.
[19] P. Baranek, J. Schamps, I. Noiret, J. Phys. Chem. B 101 (1997) 9147.
[20] J.-I. Tani, H. Kido, Comput. Mater. Sci. 42 (2008) 531.
[21] X. Gonze, J.M. Beuken, R. Caracas, F. Detraux, M. Fuchs, G.M. Rignanese, L. Sindic, M. Verstraete, G. Zerah, F. Jollet, M. Torrent, A. Roy, M. Mikami, Ph. Ghosez, J.Y. Raty, D.C. Allan, Comput. Mater. Sci. 25 (2002) 478.
[22] The ABINIT code is a common project of the Université Catholique de Louvain, Corning Incorporated, and other contributors (URL http://www.abinit.org).
[23] N. Troullier, J.L. Martins, Phys. Rev. B 43 (1991) 1993.
[24] W.H. Press, S.A. Teukolsky, W.T. Vetterling, B.P. Flannery, Numerical Recipes in Fortran 77: The Art of Scientific Computing, 2nd ed., Cambridge University Press, Cambridge, 1992, p418.
[25] H.J. Monkhorst, J.D. Pack, Phys. Rev. B 13 (1976) 5188.
[26] X. Gonze, Phys. Rev. B 55 (1997) 10337.
[27] X. Gonze, C. Lee, Phys. Rev. B 55 (1997) 10355.
[28] D. McWilliams, D.W. Lynch, Phys. Rev. 130 (1963) 2248.
[29] E. Anastassakis, E. Burstein, Solid State Commun. 9 (1971) 1525.
[30] R. Kouba, C. Ambrosch-Draxl, Phys. Rev. B 56 (1997) 14766.
[31] F. Birch, Phys. Rev. 71 (1947) 809.
[32] B.C. Gerstein, F.J. Jelinek, M. Habenschuss, W.D. Shickell, J.R. Mullaly, P.L. Chung, J. Chem. Phys. 47 (1967) 2109.
[33] P.L. Chung, W.B. Whitten, G.C. Danielson, J. Phys. Chem. Solids 26 (1965) 1753.
[34] O. Madelung, Landolt-Börnstein: Numerical Data and functional Relationships in Science and Technology, New Series, Group III, Vol. 17e, Springer-Verlag, Berlin, 1983, p. 163, 432.
[35] C. Kittel, Introduction to Solid State Physics, 7th ed., John Wiley& Sons, Inc, New York, 1996, p. 123.
[36] B.C. Gerstein, P.L. Chung, G.C. Danielson, J. Phys. Chem. Solids 27 (1966) 1161.
[37] C. Domb, L. Salter, Philos. Mag. 43 (1952) 1083.
[38] D.T. Morelli, J.P. Heremans, Appl. Phys. Lett. 81 (2002) 5126.
[39] R.J. Bruls, Ph. D. Thesis, Technische Universiteit Eindhoven, 2000.
[40] R. Bruls, H.T. Hintzen, R. Metselaar, J. Appl. Phys. 98 (2005) 126101.
[41] J.J. Martin, J. Phys. Chem. Solids 33 (1972) 1139.